

A framework of crossover of scaling law : dynamical impact of viscoelastic surface

Hirokazu Maruoka¹

¹Deep-Sea Nanoscience Research Group, Research Center for Bioscience and Nanoscience,
Research Institute for Marine Resource Utilization,
Japan Agency for Marine-Earth Science and Technology (JAMSTEC),
2-15 Natsushima-cho, Yokosuka, Kanagawa 237-0061, Japan*

(Dated: May 20, 2022)

In this paper, a crossover of scaling laws is described as a result of the interference from self-similar variable of the higher class of the self-similarity on the dynamical impact of solid sphere onto a viscoelastic surface. All the physical factors including the size of spheres, the impact of velocity are successfully summarized to the primal dimensionless numbers which construct a self-similar solution of the second kind, which represents the balance between dimensionless numbers. The self-similar solution gives two different scaling laws by the perturbation method describing the crossover. These theoretical predictions are compared with experimental results to show good agreement. It was suggested that a hierarchical structure of similarity plays a fundamental role on crossover, which offers a fundamental insight to self-similarity in general.

INTRODUCTION

“Scaling never appears by accident”[1]. Scaling law is the representation of physical law, which is expressed by a power-functional relation between physical parameters (e.g., Boyle’s law is the inverse-proportional relation between pressure and volume $P \sim V^{-1}$)

$$y = At^\alpha \quad (1)$$

in which y , t are physical parameters, A is prefactor, α is power exponent. It is quite general and basic concept in physics. It enable us to connect theory with experiment as theoretical verification is generally performed through the reference of the scaling relation obtained by the experimental observation[2]. On the other hand, one observes the case in which a scaling law transforms to another in different scale of physical variables, $y = At^\alpha \rightarrow Bt^\gamma$, which we call *crossover of scaling law*, in a wide variety of fields: the mechanics of continua[3, 4], soft matter[5], quantum physics[6], critical phenomena[7, 8] and so on. Such phenomena are very interesting for application and biology as it is expected that they can be associated with the invention of functional materials[9, 10], and may play an important role on the biological functions[11–13]. Crossover of scaling law can be formalized as *the process of transition of scaling law by the continuous change of a scale parameter*. However, the studies of crossovers generally focus on each scaling law in the extreme limit independently. As a result, they failed to formalize it as the continuous process.

The appearance of stable scaling law can be understood as an *intermediate asymptotic*[14–24], which is defined as an asymptotic representation of a function valid in a certain scale range. Barenblatt has formalized the idealization of physical theory in terms of dimensional analysis. Dimensional analysis gives a self-similar solution of which variables are dimensionless numbers con-

sisting of the physical quantities involved in the phenomena. Considering the dimensions of parameters, the scaling law of Eq. (1) can be transformed to $\Pi = y/At^\alpha$. Later the dimensionless number is related with other dimensionless numbers, say $\theta = x/t^\beta$, then $\Pi = \Phi(\theta)$. If the dimensionless function Φ converges to a finite limit, $\Phi \rightarrow \text{const}$ as $\theta \rightarrow 0$, which corresponds to *complete similarity*[25], and that a single dimensionless number is remained, an intermediate asymptotic is obtained, which results in the scaling law corresponding to Eq. (1), while it is *locally* valid in the range in which its asymptotic is maintained in this case, $y = At^\alpha$ ($\theta \ll 1$)[14]. This formalization facilitates us to understand the idealization of physics and the dimensionless numbers though his theory is limited to the case of a single scaling law and has not developed to how crossovers are formalized.

In this paper, I develop Barenblatt’s idea for crossover of scaling law. In terms of the concept of the intermediate asymptotic, it is expected that crossover must correspond to the case in which its idealization is broken. As previously mentioned, a single scaling law is obtained in the condition in which its dimensionless function converges to a finite limit, $\Phi = \text{const}$. Conversely speaking, the incomplete convergence of dimensionless function, $\Phi \neq \text{const}$, namely the interference of another dimensionless number may generate crossover of scaling law. I will demonstrate that we can understand crossover by such a framework; *crossover is generated by interference from another dimensionless number*.

To verify this framework, this work focuses on the contact mechanics[26, 27] in which crossovers of scaling laws are observed[28] depending on the form of contacts and that the physical parameters can be easily controlled. The contact phenomena are abundant in our daily life[29, 30] and industry[31]. In the present work, I show the new scaling laws on the dynamical impact of the solid sphere onto the viscoelastic surface. The viscoelastic surface is quite interesting as it can be the model in-

volving time-scale dependence[32–34]. It is also a model for the earthquake[35, 36]. The scaling relation between maximum deformation and the impact-velocity reveals a crossover depending on the impact-velocity and the size of spheres. I successfully integrate these elements into a single dimensionless number to find that the interference can be described by a self-similar solution of the second kind.

MAXWELL VISCOELASTIC FOUNDATION MODEL

Here we think about the problem in which a rigid sphere is free fall onto the viscoelastic surface (See Fig. 1). In this case, the surface is modeled by the viscoelastic-foundation model in which the stress deformation is described by foundations which are arranged in parallel[37]. Each foundation consists of a dashpot (viscous coefficient μ) and a spring (elastic modulus E), which are serially connected. In this model, the stress σ and the deformation ϵ can be related by the following differential equation with time t , $\frac{\mu}{E} \frac{d\sigma}{dt} + \sigma = \mu \frac{d\epsilon}{dt}$, which corresponds to the Maxwell model. By assuming the deformation by the impact of sphere of which deformation is δ , thickness of surface is h , the contact area is a , the deformation at position from center of sphere r can be described by $\epsilon = \frac{\delta}{h} \left[1 - \left(\frac{r}{a} \right)^2 \right]$. Assuming the main contribution is due to $\frac{d\delta}{dt} \simeq \text{const}$ for the foundation, the energy of deformation is described by

$$E_{MVF} = \frac{\pi\mu\phi R\delta^2}{h} \frac{d\delta}{dt} \left[1 - \exp\left(-\frac{Et}{\mu}\right) \right] \quad (2)$$

where R is radius of sphere, ϕ is the fraction of contact and t is contact time. $\phi = 1$ in the plane surface.

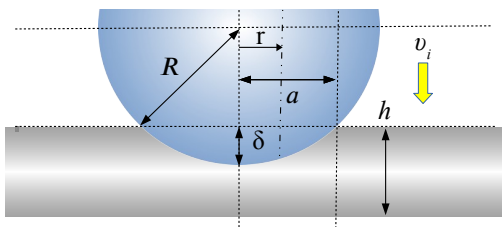


FIG. 1: (Color online) The geometrical parameters involved in the collision between elastic surface with its thickness h and solid sphere with its radius R in the impact-velocity v_i . The deformation δ and diameter of contact a are generated by the collision onto the viscoelastic surface. r is the position from center.

E_{MVF} is quite characteristic as it transforms depending on the contact time $\mu/Et = \text{De}$, Deborah number[38]. Supposing $\text{De} \gg 1$ which can be realized by the fast-time impact due to the following scaling $t_c \sim \delta_m/v_i$

where δ_m is maximum deformation, v_i is the impact-velocity and t_c is the contact time at which the deformation is maximized[39] and the relation of $\frac{d\delta}{dt} = v_i$, Taylor expansion is applied to E_{MVF} as follows; $E_{MVF} = \frac{\pi\mu\phi R\delta_m^2}{h} v_i \left[\frac{E\delta_m}{\mu v_i} - \dots \right] \simeq \frac{\pi E\phi R\delta_m^3}{h} = E_{el}$, which corresponds to the elastic energy[24, 40]. This results shows that E_{MVF} experiences a transition to fully elastic energy or the energy mixed with viscous component depending on the contact time.

Suppose that the kinetic energy of the solid ball with the density ρ is converted to E_{MVF} , we have

$$\frac{2}{3}\pi R^3 \rho v_i^2 = \frac{\pi\mu\phi R\delta_m^3}{h} v_i \left[1 - \exp\left(-\frac{E\delta_m}{\mu v_i}\right) \right]; \quad (3)$$

it is energy exchange at which the deformation is maximized.

DIMENSIONAL ANALYSIS

In order to see the self-similar structure, here I perform the dimensional analysis[41]. The physical parameters which are involved are summarized to the following function $\delta_m = f(R, h, \phi, \rho, \mu, E, v_i)$. The dimensions of the function is described as follows; $[\delta_m] = L$, $[R] = L$, $[h] = L$, $[\phi] = 1$, $[\rho] = M/L^3$, $[\mu] = M/LT$, $[E] = M/LT^2$, $[v_i] = L/T$ by LMT unit. By selecting R , ρ , E as the governing parameters with independent dimensions, which are defined as the parameters which cannot be represented as a product of the remaining parameters, following self-similar variables are defined:

$$\Pi = \frac{\delta_m}{R}, \quad \kappa = \frac{h}{R}, \quad \eta = \frac{\rho v_i^2}{E}, \quad \theta = \frac{\mu}{E^{1/2} \rho^{1/2} R} \quad (4)$$

then we have $\Pi = \Phi(\phi, \kappa, \theta, \eta)$ where η corresponds to Cauchy number, dimensionless velocity-component. To know the self-similar structure, here I check the convergence of the dimensionless function. However, the mere application of dimensional analysis is not enough to consider the self-similar structure of this model.

To go further to consider the self-similarity structure, the following solution is quite helpful,

$$\Pi = \text{const} \left(\frac{\kappa}{\phi} \right)^{\frac{1}{3}} \eta^{\frac{1}{3}} \quad (5)$$

which corresponds to Chastel-Gondret-Mongruel (CGM) solution[40, 42, 43]. We easily find that Π does not converge as η goes to infinity according to Eq. (5), which means that Eq. (5) is incomplete similarity (see Ref. [25]). However, we can make it converge by defining another self-similar variables as follows, $\Psi = \frac{\Pi^3 \phi}{\kappa \eta}$ for $\Psi = \text{const}$ as $\eta \rightarrow \infty$. Thus Ψ construct a self-similarity of different class, which corresponds to the self-similarity of the second kind[44]. By considering these structure

and applying the self-similar variable Ψ into Eq. (4), one finds the structure of similarity on this problem if we construct another self-similar variables as $Z = \frac{\Pi}{\theta\eta^{1/2}} = \frac{E\delta_m}{\mu v_i}$ then we have

$$\Psi = \frac{2}{3} \frac{Z}{[1 - \exp(-Z)]}. \quad (6)$$

Supposing $\Psi = \Phi(Z)$, Φ converges to a finite limite as Z goes to zero[45]. Therefore, equation (6) belongs to a self-similar solution of the second kind, which is defined as the power-exponents of self-similar variables cannot be determined by dimensional analysis and mathematically corresponds to a *fractal*[46].

Note that there is a hierarchical structure on the self-similar solution in Eq. (6) depending on the convergence of dimensionless function (See Fig. 2). Π , κ , θ , ϕ and η belong to a similarity-class which forms a following similarity structure: $\frac{\Pi^3\phi}{\kappa\eta} = \Phi\left(\frac{\Pi}{\theta\eta^{1/2}}\right)$. Here I call this class similarity of *the first class* as it is generated through dimensional analysis. In the first class, each parameters belong to dimensionless physical quantities. On the other hand, Ψ and Z belong to an another similarity-class to form the following similarity structure: $\Psi = \Phi(Z)$. I call this class similarity of *the second class*[47]. The variables of the second class normalizes the difference of the variables of the first class to integrate the single lines, which corresponds to the data collapse[48, 49]. In the second class, self-similar variables represents the dynamics of energy involved in the process. Ψ represents the proportion of kinetic energy and elastic energy while Z represents the proportion of viscous energy and elastic energy, which corresponds to Deborah number. One can find that $\Phi(Z)$ represents the interference of viscous components. If Z goes to 0, which can be achieved by the high-velocity impact or short-time contact, $\Phi \rightarrow \text{const}$, then we have the CGM solution, which is realized in the case in which the kinetic energy fully transforms to elastic energy. Here the convergence of $\Phi(Z)$ means the inactiveness of Z . Thus in case of $Z \ll 1$, the impact is elastically dominant, which we call elastic impact and it gives 1/3 power-law on η . However, when this idealized condition is not satisfied ($Z > 1$), which can be realized by the low-velocity impact, the viscous components $\Phi(Z)$ interferes Ψ . In this region, the viscosity contributes in the impact, then it changes scaling law. This impact corresponds to the viscoelastic impact.

We cannot see the actual scaling behavior of Π and η in viscoelastic regime from the second class. They belong to the first class and their behaviors are not simply consistent with Ψ and Z as one see $\frac{\Pi^3\phi}{\kappa\eta} = \Phi\left(\frac{\Pi}{\theta\eta^{1/2}}\right)$, which shows that Π and η are included in both variables of the higher class, Ψ and Z . In order to know the scaling-behavior of Π and η , here I apply the third term

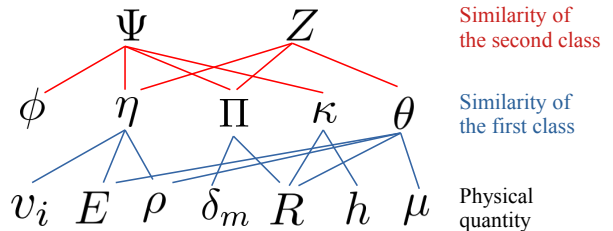


FIG. 2: (Color online) The hierarchy of self-similarity on the dynamical impact of solid sphere onto the viscoelastic surface. The solid lines signifies the composition of each dimensionless parameters. In the present study, one finds that there is a hierarchy that consists of three classes on variables ; the class to which physical quantities belong, the class to which dimensionless parameters composed by dimensional analysis belong and the class to which dimensionless parameters which is power-law monomial of dimensionless parameters to recover the convergence belong.

perturbation method[50], then we have

$$\Pi = \frac{\kappa}{54\phi\theta^2} + \left(\frac{\kappa^2}{486\phi^2\theta^3}\right)^{\frac{1}{3}} \eta^{\frac{1}{6}} + \left(\frac{2\kappa}{3\phi}\right)^{\frac{1}{3}} \eta^{\frac{1}{3}} \quad (7)$$

as $\varepsilon = \frac{1}{\theta\eta^{1/2}} \rightarrow 0$ [51].

As we can see, Eq. (7) includes two different power exponents as $\eta^{1/3}$ and $\eta^{1/6}$, which suggests that intermediate asymptotics appear depending on θ , η or Z . In case of the impact of high velocity and/or smaller sphere, which corresponds to $\eta \gg 1$ and/or $\theta \gg 1$ and $Z \ll 1$, $\eta^{1/3}$ is dominant. Conversely in the region of viscoelastic impact in which $Z > 1$, realized by low-velocity $\eta \ll 1$ and/or the impact of larger sphere $\theta \ll 1$, $\eta^{1/6}$ is dominant while the intermediate behavior may be realized in $Z \sim 1$.

EXPERIMENT

To show the validity of the theory, the experiments have been performed using a viscoelastic surface made of polydimethylsiloxane (PDMS) (Fig. 3). The PDMS (SILPOTTM 184 W/C, DOW) surface was prepared by mixing curing agent and base by the proportion of 1 : 40 and pour into the mold. After leaving for 3 hr 30 min at 60 C°, the surface was solidified, of which thickness $h = 7.5$ mm, the fraction of contact $\phi = 1$, elastic modulus $E \simeq 0.57$ MPa and viscous coefficient $\mu = 117$ Pa · s. The elastic modulus and viscous coefficient were estimated by fitting the experimental results. The PDMS surface was coated with grease (WD-40) to prevent the adhesive effect. The metallic ball (Tsubaki Nakashima co., ltd., SUJ2) was suspended by the electromagnet (ESCO Co.,Ltd., EA984CM-1) of which magnet

force is controlled. Once the ball is released from the electromagnet, it starts to free fall and collides with the PDMS surface (Fig. 4)[52]. After the contact of surface, it reaches to the maximum deformation δ_m then rebounds to release from surface again.

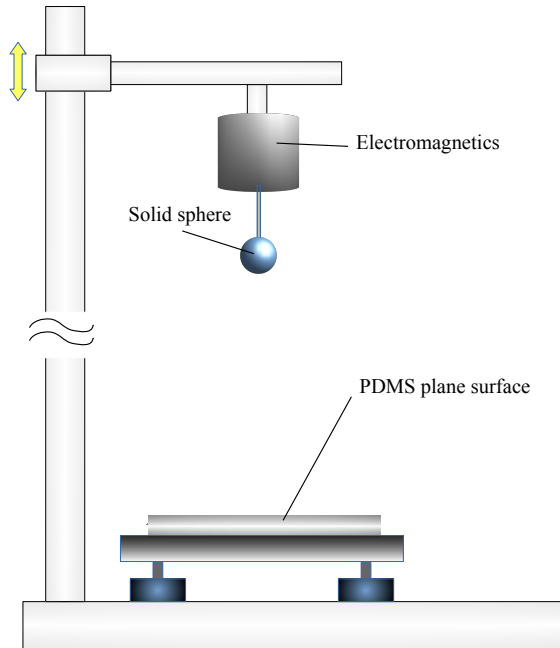


FIG. 3: (Color online) Sketch of experimental setup. The solid sphere is suspended by an electromagnet. The velocity of impact is adjusted by changing the height of the part in which the sphere is suspended. The sphere ($R = 3.0, 4.0, 5.0, 6.0, 7.0$ and 8.0 mm, $\rho = 7800 \text{ kg} \cdot \text{m}^{-3}$) is dropped onto the PDMS plane surface ($\phi = 1, h = 7.5$ mm).

The processes are observed by high speed camera (FASTCAM SA1.1, 768×768 pixel, 10000 fps). The size of sphere R is differed as 3.0, 4.0, 5.0, 6.0, 7.0 and 8.0 mm, of which density $\rho = 7800 \text{ kg} \cdot \text{m}^{-3}$. The collision experiments were performed for 6 times in each conditions. The information of velocity, maximum deformation, contact time and so on were extracted from the movies by image analysis which is programmed by Python using Open CV. Using these numerical estimations, the dimensionless numbers of the self-similarity of the first class, and the second class were calculated.

DISCUSSION

Figure 5 shows the self-similar variables in different self-similarity class. Figure 5 (a - f) demonstrates the self-similarity of the first class, which is the power-law relation between Π and η in different size of spheres while Figure 5 (g) demonstrates the self-similarity of the sec-

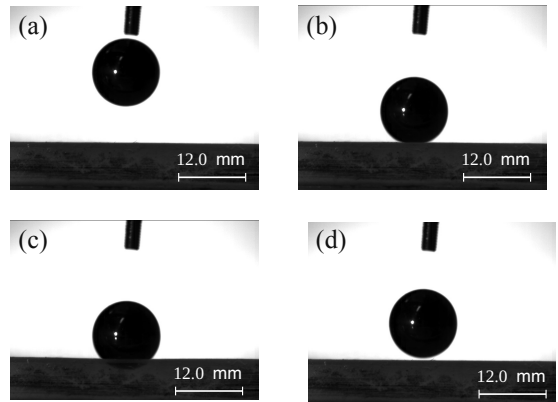


FIG. 4: (Color online) The images of the dynamical impact of sphere ($R = 6.0$ mm) onto the elastic surface at $v_i = 370$ mm/s with the frame rate for 10000 images per second and the resolution of 768×768 pixels. (a) The image before impact. (b) The moment of contact. (c) The moment of maximum deformation at $t = 11$ ms after contact. (d) The image releasing from surface after contact. The movie is uploaded as Supplemental Material [1].

ond class, which is their Ψ and Z . As we can see, the plots of Π and η reveal gradually different scaling law from $R = 3.0$ mm to 8.0 mm. Equation (7) predicts that Π and η have different power law depending on θ and η , finally summarized to $\Phi(Z)$. As the prediction mentioned in previous section suggests, the impacts of the smaller spheres ($R = 3.0, 4.0$ mm) which tends to have smaller Z follow $1/3$ power-law, which corresponds to elastic impact (Fig. 5 (a, b)). $\Phi(Z)$ belonging to the plots of $1/3$ power-law shows the smaller Z and tendency to convergence to a finite limit, which signifies that $\Phi(Z)$, viscous component hardly contribute. On the other hand, larger spheres ($R = 7.0, 8.0$ mm) reveal different power-law, which is closer to $1/6$ power-law in low-velocity (Fig. 5 (e, f)). The plots revealing $1/6$ power-laws belong to the larger Z and Ψ increases in Fig. 5 (g), which means that viscous component $\Phi(Z)$ contributes and it is viscoelastic impacts. The dash-dots lines which are described by Eq. (7) are consistent with the power-law behavior of the plots. The plots of intermediate size of spheres ($R = 5.0, 6.0$ mm) reveals slightly intermediate scaling law between $1/3$ and $1/6$ though this behavior is well described by the Eq. (7). All these plots roughly follow the line described by the self-similar solution of Eq. (6) in Fig. 5 (g).

The deviation of plots from the theoretical lines may be originated from the technical reason and the theoretical assumption. In the model, the interaction of the surface, adhesion effect are not considered. To realize this assumption, the adhesion effect was decreased by coating grease though it may not be enough to remove these

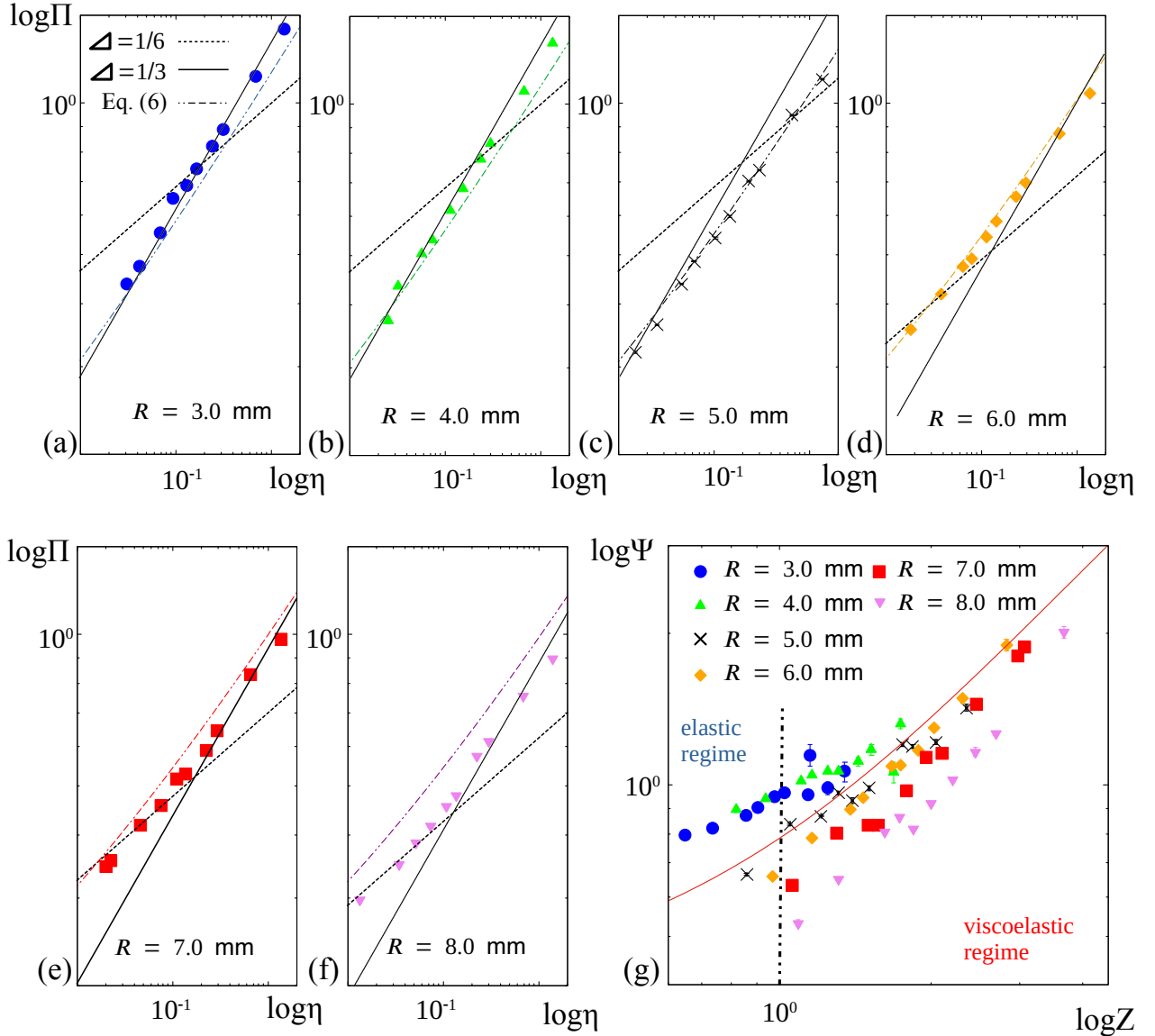


FIG. 5: (Color online) The different hierarchical structure of self-similarity. (a) - (f) Self-similarity of the first class : the power law relations Π and η in different size of sphere. The dashed lines indicates the slope of $1/6$, the solid line indicates the slope of $1/3$ and colored dot-dashed line indicates Eq. (7) in each size of spheres. (g) Self-similarity of the second class : the plots between Ψ and Z . $R = 3.0$ mm (\bullet), 4.0 mm (\blacktriangle), 5.0 mm (\times), 6.0 mm (\blacklozenge), 7.0 mm (\blacksquare) and 8.0 mm (\blacktriangledown) where $\Pi = \delta_m/R$, $\eta = \rho v_i^2/E$, $\Psi = \frac{\Pi^3 \phi}{\kappa \eta} = \frac{\delta_m^3 E}{R^2 h \rho v_i}$ and $Z = \frac{\Pi}{\theta \eta^{1/2}} = \frac{E \delta_m}{\mu v_i}$. The red line in Figure (g) is Eq. (6).

interaction completely, which may result in the dependence on the size of spheres. Furthermore, the foundation model considers only vertical deformation though it is not completely satisfied actually, which might make difference. Even though one sees some deviation originated from these considerations, we can say that the scaling behaviors were well described by theoretical lines, which demonstrates the good consistency.

In this model, the foundation model is applied which considers only vertical deformation, which is also applied to the previous work in which a rectangular pillar surface is used[24]. The application of the foundation model is justified by the experimental results of $R = 3.0, 4.0$ mm in Fig. 5 in which the impact is fully elastic as the scaling result corresponds to the CGM solution. In this work, the surface is much more viscoelastic, and the

viscous components is origin of the crossover while the inertia-effect played a roll in previous work. However, the framework that crossover is generated by another dimensionless number is the same though this work succeeded to describe explicitly the dimensionless function Φ , which make it possible to discuss the self-similar structure clearly.

The model assumes the main contribution is due to $\frac{d\delta}{dt} = \text{const}$. This assumption is well justified by the observation (see Fig. S2)[53]. The time evolution of deformation shows $\frac{d\delta}{dt} = v_i$ which is persists in a certain region, then the speed of deformation steeply decreases in the end. The same behaviors are observed in both elastic and viscoelastic impact. Furthermore, if one considers the time-dependence of the speed of deformation as $\frac{d\delta}{dt} = v_i + f(t)$ in which $f(t)$ can be expanded in regard to t and if it is well ordered, it is found that the time-dependence effect of $f(t)$ does not change the perturbation result[53]. Experimentally the coefficient between t_c and δ_m/v_i is found then we used a following relation on the calculation ; $1/De \simeq 1.90Z$. However, these effect did not change the scaling relation and was only reflected on the coefficient (See Fig. S3)[54].

Falcon et al. discussed the roll of gravity on the repeated bouncing ball[55]. In this work, as the maximal deformation and the impact velocity, which is determined by the energy exchange, are focused, the roll of gravity is not apparent. However, it is indirectly related as the impact-velocity while the gravity fields is constant in this experiment. This effect does not make difference on the results, which is the limitation of this work. On the other hand, in the static contact, it is determined by the balance between the gravity force and the elastic force, the roll of gravity should be considered. It suggests that the information which can be extracted through the dynamical impact and static impact can be fundamentally different. This point is expected to be future interest as it can be applied to the sensing technique.

Focusing on the phenomenon itself, E_{MVF} reveals an interesting feature as it transforms its form qualitatively depending on Z . Such a behavior does not appear from Kelvin Voigt model, which is another model for viscoelastic materials and consists of the spring and dash pot are parallelly connected, though Kelvin Voigt model does not make crossover. It is not appropriate for this problem.

The analysis based on the different class of self-similarity gives different view of the process. The scaling behavior of the first class, which is apparent to our interest, is not clear within this class as the actual behavior of the scaling laws are finally determined by the competition of the self-similar variables of the second class, which is expressed as the self-similar solution : $\Psi = \Phi(Z)$. This relation is the key to the framework of crossover of scaling law which is proposed in introduction. When $\Phi = \text{const}$, CGM solution is obtained as an intermediate asymptotics then $\Pi \sim \eta^{1/6}$. However, in case of $\Phi \neq \text{const}$, which

means the interference of another dimensionless number Z , another scaling law appears, $\Pi \sim \eta^{1/6}$. This is the fundamental mechanism of the crossover of scaling law in this problem. Therefore, the transition of the scaling law, which corresponds to crossover, cannot be explained without the consideration of this hierarchical structure. $\Phi(Z)$ does not only qualitatively decide the crossover but also it numerically expresses the balance between the dimensionless numbers. This numerical balance accurately decides the balance of coefficients of Eq. (7), which enables us to describe the exact behaviors of crossover more accurately.

It should be noted that the behavior of variables of the higher class does not always correspond to the one of variables of the lower class. As the variables of the higher class consist of the variables of the lower class. In case that the interesting variables are included in several variables of the higher class, the variables are not independent one another, which requires the perturbation method.

It is expected that the framework which was shown in this paper is not limited to this present work. All the stable scaling laws should be intermediate asymptotics in which dimensionless functions converge. Thus the transition of scaling laws must be given by the violation of this idealization. Yasuda et al. also reported the primal dimensional number to change the scaling laws[56]. Barenblatt reported the dependence of power exponents by another dimensionless numbers[57, 58] though in these cases the exact form of dimensionless function Φ were unclear and the hierarchy was not focused on. In the present work, I succeeded to identify the exact form of dimensionless functions. The insights in the present work suggested that the investigation of hierarchy of the higher class can be the clue to describe crossover.

Finally, the combination of dimensionless number listed on Eq. (4) is not the only possible selection. However, this combination is plausible in terms of the perturbation. It suggests that the selection of dimensionless numbers is not arbitrary as it is related with the strategy of perturbation. $\theta = \frac{\mu}{E^{1/2}\rho^{1/2}R}$, appearing naturally in this problem and playing an essential role, is also an interesting dimensionless number as it can be expressed as $\theta = \text{Re}/\text{Ca}^{1/2}$ in which Re is Reynolds number and Ca is Cauchy number. θ is here indicates the proportion of viscosity, elasticity and inertia.

CONCLUSION

The above discussion with experimental results confirms the validity of Eq. (6) with Eq. (7) as the fundamental equation of this problems. In this paper, I have succeeded to obtain the self-similar solutions governing the exact behavior of crossover of scaling law theoretically, which was verified experimentally. Then I have

succeeded to demonstrate that the *crossover of scaling is generated by the interference of the self-similar variables of the higher class*, which corresponds to the framework mentioned in the introduction.

The method exercised in this work is unique in terms of methodology. The degree of this interference is quantitatively and qualitatively estimated and it enable us to describe crossover as the continuous process more accurately. This accuracy was guaranteed by the coefficients of the different scaling laws which was given by the self-similar solution of the second class, which suggests that the coefficients are essential on the accurate description of crossover.

Finally, intermediate asymptotics is the *locally* valid asymptotic expression while we have found that this locality is governed by the self-similar solution of the higher class in this paper. This framework is simple and expected to be quite general in physics. Besides, it is similar to critical phenomena in which the transition of phase is generated by the continuous parameter variation. Therefore, the present work supplies interesting insights for the concept of self-similarity, nonequilibrium theory and critical phenomena, for a wide variety of fields in physics in general.

ACKNOWLEDGEMENT

The author wishes to thank D. Nishiura for technical assistance of the experiments, G. Li for technical advice of experimental setup, D. Matsuoka for technical advice for the algorithm of the program for image analysis, S. Okada, E. Barbieri and Y. Kawamura for helpful discussion and many support for the experiment. He is appreciated with the members at MAT (Center for Mathematical Science and Advanced Technology) seminar at JAMSTEC for fruitful discussion.

* Electronic address: maruokah@jamstec.go.jp; Electronic address: hmaruoka1987@gmail.com

- [1] G. I. Barenblatt, *Scaling* (Cambridge University Press, 2003) p.1.
- [2] P.-G. de Gennes, *Scaling Concepts in Polymer Physics* (Cornell University Press, 1979).
- [3] M. Yokota, K. Okumura, Dimensional crossover in the coalescence dynamics of viscous drops confined in between two plates, *Proc. US Nat. Acad. Sci.* **108**, 6395 (2011).
- [4] M. Murano and K. Okumura, Rising bubble in a cell with a high aspect ratio cross-section filled with a viscous fluid and its connection to viscous fingering, *Phys.Rev.Res.*, **2**, 013188 (2020).
- [5] G. C. Berry and T. G. Fox, The Viscosity of Polymers and Their Concentrated Solutions, *Adv. Polym. Sci.* **5**, 261 (1968).
- [6] R. Vasseur, K. Trinh, S. Haas, and H. Saleur, Crossover Physics in the Nonequilibrium Dynamics of Quenched Quantum Impurity Systems, *Phys. Rev. Lett.* **110**, 240601 (2013).
- [7] E. Lujiten and H. W. J. Blöte, Crossover scaling in two dimensions, *Phys. Rev. E* **56**, 6540 (1997).
- [8] S. Lübeck, Universal Behavior of Crossover Scaling Functions for Continuous Phase Transitions, *Phys.Rev.Lett.*, **90**, 210601 (2003).
- [9] W. J. Parnell and R. De Pascalis, Soft metamaterials with dynamic viscoelastic functionality tuned by pre-deformation, *Phil. Trans. R. Soc. A*, **377**: 20180072, (2019).
- [10] R. N. Glaesener, J.-H. Bastek, F. Gonon, V. Kannan, B. Telgen, B. Spöttling, S. Steiner, D. M. Kochmann, Viscoelastic truss metamaterials as time-dependent generalized continua, *J. Mech. Phys. Solids.*, **156** 104569, (2021).
- [11] The discontinuous transition of biological function by the change of physical parameters are discussed as "Funktionswandel" in the following book: V. v. Weizsäcker, *Der Gestaltkreis. Theorie der Einheit von Wahrnehmen und Bewegen* (Suhrkamp, 1997).
- [12] B. Bhushan, Biomimetics: lessons from nature — an overview, *Phil. Trans. R. Soc.*, **367** 1445, (2009).
- [13] U. Krohs, The Epistemology Biomimetics: The Role of Models and of Morphogenetic Principles, *Perspective on Science*, **29** 583, (2021).
- [14] See Supplemental Material for Intermediate asymptotics.
- [15] See Ref. [1] pp.60 - 65.
- [16] G. I. Barenblatt, *Scaling, self-similarity, and intermediate asymptotics* (Cambridge University Press, 1996) pp.86-94.
- [17] G. I. Barenblatt, *Flow, Deformation and Fracture* (Cambridge University Press, 2014).
- [18] G. I. Barenblatt and Ya. B. Zeldovich, Self-similar solutions as intermediate asymptotics, *Ann. Rev. Fluid Mech.* **4**, 285 (1972).
- [19] N. Goldenfeld, O. Martin and Y. Oono, Intermediate asymptotics and renormalization group theory, *J. Sci. Comput.* **4**, 355 (1989).
- [20] N. Goldenfeld, *Lecture On Phase Transitions And The Renormalization Group* (Addison-Wesley Publishing Company, 1992) Ch.10.
- [21] Y. Oono, *The Nonlinear World* (Springer, 2013) Ch.3.
- [22] M. Benzaquen, T. Salez, E. Raphaël, Intermediate asymptotics of the capillary-driven thin-film equation, *Eur. Phys. J. E* **36** 82, (2013).
- [23] O. Bäümchen, M. Benzaquen, T. Salez, J. D. McGraw, M. Backholm, P. Fowler, E. Raphaël, K. D.-Veress, Relaxation and intermediate asymptotics of a rectangular trench in a viscous film, *Phys.Rev.E* **88**, 035001 (2013).
- [24] H. Maruoka, Intermediate asymptotics on dynamical impact of solid sphere on mili-textured surface, *Phys.Rev.E* **100**, 053004 (2019).
- [25] See Refs. [1] (pp. 82-87), [16] (pp. 145-160) and [17] (pp. 153-163). The case in which dimensionless function obtained by dimensional analysis $\Phi(\xi, \eta)$ converges to a finite limit as $\eta \rightarrow 0$ or ∞ corresponds to *complete similarity* or *similarity of the first kind* in η while the case in which the complete similarity is not satisfied but the convergence of dimensionless function is recovered by constructing the new self-similar variables as Π/η^ζ and ξ/η^ϵ , corresponds to *incomplete similarity* or *similarity of*

- the second kind.* See Supplemental Material for Complete similarity and incomplete similarity.
- [26] H. Hertz, *Miscellaneous Papers* (MacMillan & CO, 1896) p 146.
- [27] K. L. Johnson, *Contact mechanics* (Cambridge University Press, 1985).
- [28] L. Kogut and I. Etsion, Elastic-Plastic Contact Analysis of a Sphere and a Rigid Flat, *J. Appl. Mech.* **69**, 657 (2002).
- [29] R. W. Carpick, Approximate models of interacting surfaces competed against a supercomputer solution, *Science* **359**, 38 (2018).
- [30] A. M. Nathan, J. J. Crisco, R. M. Greenwald, D. A. Russell and L. V. Smith, A comparative study of baseball bat performance, *Sports Eng.* **13**, 153 (2011).
- [31] I. G. Goryacheva, *Contact Mechanics in Tribology* (Kluwer Academic Publishers, 1998).
- [32] S. C. Hunter, The Hertz problem for a rigid spherical indenter and a viscoelastic half-space, *J. Mech. Phys. Solids*, **8** 4, 219-234 (1960).
- [33] J.-M. Hertzsch, F. Spahn, N. V. Brilliantov, On Low-Velocity Collisions of Viscoelastic Particles, *J. Phys. II France* **5** 1725-1738 (1995).
- [34] N. V. Brilliantov, A. V. Pimenova and D. S. Goldobin, A dissipative force between colliding viscoelastic bodies: Rigorous approach, *Eur. Phys. Lett.*, **109** 1, 14005 (2015).
- [35] H. Suito, Importance of rheological heterogeneity for interpreting viscoelastic relaxation caused by the 2011 Tohoku-Oki earthquake, *Earth, Planets and Space* **69**:21 (2017).
- [36] R. Agata, S. D. Barbot, K. Fujita, M. Hyodo, T. Inuma, R. Nakata, T. Ichimura, T. Hori, Rapid mantle flow with power-law creep explains deformation after the 2011 Tohoku mega-quake, *Nat. Commun.* **10**, 1385 (2019).
- [37] See Ref. [27] (pp.104-106).
- [38] M. Reiner, The Deborah Number, *Physics Today* **17**, 62 (1964).
- [39] See Ref. [27] p. 353.
- [40] T. Chastel, P. Gondret and A. Mongruel, Texture-driven elastohydrodynamic bouncing, *J. Fluid Mech.* **805**, 577 (2016).
- [41] See Refs. [1] (pp. 91-93), [16] (pp.159-160).
- [42] T. Chastel and A. Mongruel, Sticking collision between a sphere and a textured wall in a viscous fluid, *Phys. Rev. Fluids* **4**, 014301 (2019).
- [43] A. Mongruel and P. Gondret, Viscous dissipation in the collision between a sphere and a textured wall, *J. Fluid Mech.* **896** (2020).
- [44] See Refs. [1] (pp.82-91), [16] (pp.151-159) and [17] (pp. 153-163). See Supplemental Material for Complete similarity and incomplete similarity.
- [45] $\Phi(Z)$ looks like an indeterminate form as $Z \rightarrow 0$ though the convergence can easily be verified by L'Hôpital's rule. See Supplemental Material for The convergence of Eq. (6).
- [46] B. B. Mandelbrot, *The fractal geometry of nature* (Macmillan, 1983).
- [47] Barenblatt formulated the category for the first kind and the second kind as the property of convergence of dimensionless function. However, one can find that there exists a hierarchy that consists of three classes on variables : the class to which physical quantities belong, the class to which dimensionless parameters composed by dimensional analysis belong and the class to which dimensionless parameters which is power-law monomial of dimensionless parameters to recover the convergence belong. In order to refer these classes depending on which kind of parameters belong, here I invent the terms *the first class* and *the second class*.
- [48] S. M. Bhattacharjee and F. Seno, A measure of data collapse for scaling, *J. Phys. A: Math. Gen.* **34** 6375, (2001).
- [49] H. Nakazato, Y. Yamagishi and K. Okumura, Self-similar dynamic of air film entrained by a solid disk in confined space: A simple prototype of topological transitions, *Phys.Rev.Fluid*, **3**, 054004 (2018).
- [50] M. H. Holmes, *Introduction to Perturbation Methods* (Springer 2nd ed., 2013) pp.22-27.
- [51] See Supplemental Material for the derivation of Eq. (7).
- [52] See Supplemental Material at [] for a movie of a dynamical impact of solid sphere ($R = 6$ mm) onto the viscoelastic surface at $v_i = 370$ mm/s with the frame rate for 10000 image per second and the resolution of 768×768 pixels.
- [53] See Supplemental Material for The time evolution of deformation.
- [54] See Supplemental Material for the The relation between the Deborah number and Z .
- [55] E. Falcon, C. Laproche, S. Fauve, C. Coste, Behavior of one inelastic ball bouncing repeatedly off the ground, *Eur. Phys. J. B.*, **3**, 45- 57 (1998).
- [56] T. Yasuda, N. Sakumichi, U. Cheng, T. Sakai, Universal Equation of State Describes Osmotic Pressure throughout Gelation Process, *Phys.Rev.Lett.* **125**, 267801 (2020).
- [57] G. I. Barenblatt, A. J. Chorin and V. M. Prostokishin, A model of a turbulent boundary layer with a nonzero pressure gradient, *Proc. US Nat. Acad. Sci.* **99**, 5572 (2002).
- [58] G. I. Barenblatt and L. R. Botvina, Incomplete similarity of fatigue in a linear range of crack growth, *Fatigue Eng. Mater. Struct.* **3**, 193 (1981).

Supplemental materials to the manuscript of A framework of crossover of scaling law : dynamical impact of viscoelastic surface

INTERMEDIATE ASYMPTOTICS

In this section, I briefly explain the concept of *intermediate asymptotics* which is formalized by Barenblatt[1–4] by using a simple example. Intermediate asymptotics is an asymptotic representation of a function valid in a certain range of independent variables, which corresponds to a kind of the formalization of the idealization which accompanies with the construction of physical model. To understand this concept, the following problem of dimensional analysis might be helpful. Imagine that the circle is pictured on the surface of the sphere (See Fig. S1). In this problem, the physical parameters that are involved are the surface area of circle S , radius of the circle r and the radius of sphere R . Here we would like to know the scaling behavior between S and r . Therefore we assume the functional relation as follows: $S = f(r, R)$.

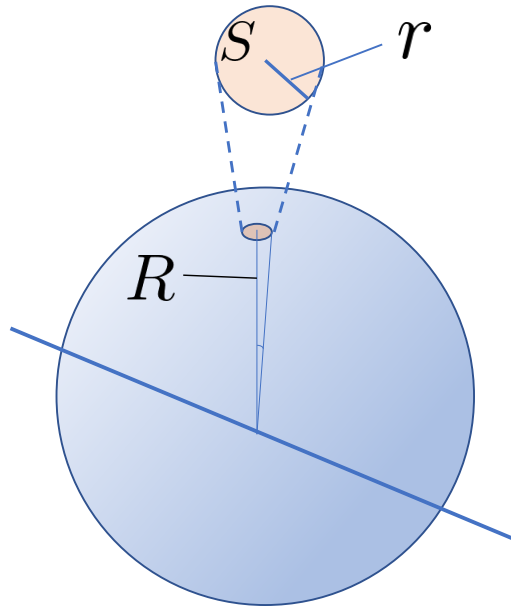


FIG. S1: (Color online) A circle of which radius is r and surface area is S , described on a sphere of which radius is R .

In this case, we attempt to obtain the exact scaling behavior by dimensional consideration. According to dimensional analysis, as the dimension of physical parameters $[S] = L^2$, $[r] = L$ and $[R] = L$, selecting r as a governing parameter of independent dimension, we have the following dimensionless function,

$$\Pi = \Phi(\theta) \quad (S1)$$

where $\Pi = \frac{S}{r^2}$ and $\theta = \frac{r}{R}$. Eq. S1 suggests that we expect the following scaling relation, $S \sim r^2$, if Π is constant. However, we easily find that this guess depends on the behavior of Φ .

By the geometrical consideration, in this case we can calculate the exact form of Φ as follows,

$$\Phi(\theta) = 2\pi \frac{1 - \cos\theta}{\theta^2}. \quad (S2)$$

To know the behavior of Φ in the case in which $\theta \rightarrow 0$, which corresponds to the increase of R or the decrease of r , Taylor expansion is applied to Eq. (S2) then we have,

$$\Pi = \Phi(\theta) \simeq \pi - \frac{\pi}{12}\theta^2 \cdots + \xrightarrow{\theta \rightarrow 0} \pi. \quad (S3)$$

As Eq. (S3) shows, Φ converges to a finite limit π , then we have a following intermediate asymptotics as $\Pi = \frac{S}{r^2}$,

$$S = \pi r^2 \quad (0 < r \ll R) \quad (\text{S4})$$

as far as the asymptotic condition $\theta \ll 1$, corresponding to $0 < r \ll R$, is satisfied.

Note that the scaling law Eq. (S4) is valid in the scale range ($0 < r \ll R$), in which the circle is significantly smaller than the sphere. Therefore, Eq. (S4) is an asymptotic expression which is valid in the certain range of variable r . This scaling law formalized *locally* is an intermediate asymptotic in this problem. Barenblatt insisted that this framework is applicable to the construction of physical model.

The important point of this concept is that every physical problem has dimension and can be applied dimensional analysis to obtain dimensionless function Φ . By considering the convergence of Φ , some self-similar variables can be selected to have the idealized solution effectively and practically as the convergence of Φ can be verified by the experimental or simulational results even if the exact form of Φ is not obtained. This procedure give rise to the strategy of Barenblatt as it is formalized in the recipe[5].

The second important point is that this process, in which one screens the self-similar variables of Φ depending on their convergence, corresponds to idealization of the problems. More or less, all the physical models involve idealizations such as ignorance of friction force, ignorance of quantum or relativity effect. All these assumption corresponds to the idealizing process of dimensionless function. For example, ideal gas equation can be considered as an intermediate asymptotic valid in the range where the volume of molecules b and the molecular interaction a are negligible on van der Waals equation as follows,

$$p = \frac{nRT}{V - nb} - \frac{an^2}{V^2} \rightarrow \frac{nRT}{V} \quad \left(\frac{an^2}{V^2} \ll p \ll \frac{RT}{b} \right). \quad (\text{S5})$$

This idealizing scale range is satisfied as far as $\Pi_a = \frac{an^2}{pV^2} \ll 1$ and $\Pi_b = \frac{pb}{RT} \ll 1$. The interested readers may refer to Ref.[6] for further discussion related with phenomenology, renormalization and asymptotic analysis on physics.

This concept suggests that every physical theory is *locally* valid. This localization is quantitatively and qualitatively formalized by the intermediate asymptotics. In the present work, the author focuses on this point and consider the case of the transition of this *locality*.

COMPLETE SIMILARITY AND INCOMPLETE SIMILARITY

In this section, I briefly explain *complete similarity* and *incomplete similarity*, as well as the *self-similarity of the first kind* and the *self-similarity of the second kind* [7]. They are the category in terms of the convergence of dimensionless function. Zeldovich noted that there exists the type of self-similarity[8]. As the previous section showed, the self-similar solution is obtained by dimensional analysis. Supposing that a certain physical function,

$$y = f(t, x, z) \quad (\text{S6})$$

in which y , t , x and z are certain physical quantities which have physical dimensions. Selecting t as a governing parameter with independent dimension, which is defined as physical parameters which cannot be represented as a product of the remaining parameters, then we apply dimensional analysis to have

$$\Pi = \Phi(\eta, \xi) \quad (\text{S7})$$

where $\Pi = y/t^\alpha$, $\eta = x/t^\beta$ and $\xi = z/t^\gamma$. α , β and γ can be fully determined by the consideration of dimension of parameters through dimensional analysis.

If Φ converges to a finite limit as ξ goes to zero or infinity, this case corresponds to *complete similarity* or *similarity of the first kind* in the similarity parameter ξ . In this case, ξ can be excluded on the consideration and we have an intermediate asymptotics. Once η and ξ both satisfy the complete similarity then $\Phi \rightarrow \text{const}$ as $\eta \gg 1$ and $\xi \gg 1$, then we have a following intermediate asymptotic, $y = \text{const } t^\alpha$ ($0 < t \ll x^{1/\beta}$, $0 < t \ll z^{1/\gamma}$). When the self-similar variables satisfies the condition of complete similarity, $\Pi = \Phi(\xi, \eta)$ is corresponds to a *self-similar solution of the first kind*. In the previous section, as Eq. (S3) shows, the dimensionless function converges to a finite limit, therefore the problem belongs to complete similarity and Eq. (S1) is a self-similar solution of the first kind.

On the other hand, in the case in which the complete similarity is not satisfied, namely Φ does not converge to a finite limit as η goes to zero or infinity, but the convergence is recovered by constructing new self-similar variables as

the power-law monomial using dimensionless variables, this case corresponds to *incomplete similarity* or *similarity of the second kind*. In this case, we may have the following self-similar solution, which is called *self-similar solution of the second kind*,

$$\Psi = \Phi(Z) \quad (\text{S8})$$

where $\Psi = \Pi/\eta^\zeta$ and $Z = \xi/\eta^\epsilon$.

The first important point is that the power exponent ζ and ϵ cannot be determined by dimensional analysis in case of the second kind while it is possible in case of the first kind. We may occasionally determine ζ and ϵ by the method for nonlinear eigenvalue problems[9] or renormalization group theory[10, 11] though we may consider them as simply empirical numbers[12]. It was suggested that self-similarity of the second kind corresponds to *fractal*[13, 14], which was elaborated by Mandelbrot. The fractal is a geometrical object which is lacking in a characteristic length. If the objects possess a certain characteristic length, the scale of the object is apparent by scale transformation. On the other hand, the scale of fractal objects is not apparent but self-similar as the scale transformation. Such a geometrical property corresponds to the divergence of dimensionless function in dimensional analysis.

The second important point is that there exists a hierarchy of self-similarity. Note that we can find a parallelism between the first kind and the second kind. Dimensional analysis transforms $y = f(t, x, z)$ to $y/t^\alpha = \Phi(x/t^\beta, z/t^\gamma)$ while $\Pi = \Phi(\eta, \xi)$ is transformed to $\Pi/\eta^\zeta = \Phi(\xi/\eta^\epsilon)$ in case of the second kind. In the present study, I focused on this hierarchy though the first kind and the second kind refer to the property of the convergence of dimensionless function, not to the classes to which dimensionless parameters belong. Thus, I introduced a word, *class* to characterize the hierarchical structure.

By considering the convergence of the self-similar variables, the self-similar structure of the problem are explored, and intermediate asymptotics is finally obtained. Depending on the type of similarity, the asymptotics is called *intermediate asymptotics of the first kind* or *intermediate asymptotics of the second kind*.

THE CONVERGENCE OF EQ. (6).

Eq. (6) is seemingly an indeterminate form as $Z \rightarrow 0$ though it converges to a finite limit as follows. Using L'Hôpital's rule, then we have

$$\lim_{Z \rightarrow 0} \frac{2}{3} \frac{Z}{1 - e^{-Z}} = \lim_{Z \rightarrow 0} \frac{2}{3} \frac{(Z)'}{(1 - e^{-Z})'} = \frac{2}{3}. \quad (\text{S9})$$

THE DERIVATION OF EQ. (7)

According to Eq. (6), in the self-similarity of the first class, we have

$$\frac{\Pi^3 \phi}{\kappa \eta} = \frac{2}{3} \frac{\frac{\Pi}{\theta \eta^{1/2}}}{\left[1 - \exp\left(-\frac{\Pi}{\theta \eta^{1/2}}\right)\right]}. \quad (\text{S10})$$

By multiplying $\frac{\kappa \eta}{\Pi^3 \phi}$ and we have the following form from Eq. (S10)

$$\frac{2}{3} = \Pi^2 \theta \frac{\phi}{\kappa \eta^{1/2}} \left[1 - \exp\left(-\frac{\Pi}{\theta \eta^{1/2}}\right)\right]. \quad (\text{S11})$$

In order to see the actual behavior of Π , I applied the third term perturbation method. As it belongs to the problem of the singular perturbation[15], therefore here we assume

$$\Pi = \frac{1}{\varepsilon^\gamma} (\Pi_0 + \varepsilon^\alpha \Pi_1 + \varepsilon^{2\alpha} \Pi_2 + \dots) \quad (\text{S12})$$

where γ and α are constant, $\varepsilon = 1/\theta \eta^{1/2}$.

By applying the Taylor expansion on the exponential part and substituting Eq. (S12) into Eq. (S11), we have

$$\begin{aligned} & \theta^2 \frac{\phi}{\kappa} \varepsilon \Pi^2 \left\{ \varepsilon \Pi - \frac{1}{2} \varepsilon^2 \Pi^2 + \frac{1}{6} \varepsilon^3 \Pi^3 \dots \right\} = \frac{2}{3} \\ \Leftrightarrow & \theta^2 \frac{\phi}{\kappa} \varepsilon^{1-2\gamma} \left(\Pi_0^2 + 2\varepsilon^\alpha \Pi_1 \Pi_0 + 2\varepsilon^{2\alpha} \Pi_2 \Pi_0 + \varepsilon^{2\alpha} \Pi_1^2 + \dots \right) \{ \varepsilon^{1-\gamma} (\Pi_0 + \varepsilon^\alpha \Pi_1 + \varepsilon^{2\alpha} \Pi_2 + \dots) \\ & - \frac{1}{2} \varepsilon^{2-2\gamma} (\Pi_0^2 + 2\varepsilon^\alpha \Pi_1 \Pi_0 + 2\varepsilon^{2\alpha} \Pi_2 \Pi_0 + \varepsilon^{2\alpha} \Pi_1^2 + \dots) + \frac{1}{6} \varepsilon^{3-3\gamma} (\Pi_0^3 \dots) \dots \} = \frac{2}{3} \end{aligned} \quad (\text{S13})$$

as $\varepsilon \rightarrow 0$.

To balance each terms, we find that $\gamma = 2/3$ and $\alpha = 1/3$ then we obtain,

$$\begin{aligned} & \theta^2 \frac{\phi}{\kappa} \left(\Pi_0^2 + 2\varepsilon^{1/3} \Pi_1 \Pi_0 + 2\varepsilon^{2/3} \Pi_2 \Pi_0 + \varepsilon^{2/3} \Pi_1^2 + \dots \right) \{ \Pi_0 + \varepsilon^{1/3} \Pi_1 + \varepsilon^{2/3} \Pi_2 + \dots \\ & - \frac{1}{2} \varepsilon^{1/3} \left(\Pi_0^2 + 2\varepsilon^{1/3} \Pi_1 \Pi_0 + 2\varepsilon^{2/3} \Pi_2 \Pi_0 + \varepsilon^{2/3} \Pi_1^2 + \dots \right) + \frac{1}{6} \varepsilon^{2/3} (\Pi_0^3 \dots) \dots \} = \frac{2}{3}. \end{aligned} \quad (\text{S14})$$

From this we have

$$\begin{aligned} O(1) \Leftrightarrow & \theta^2 \frac{\phi}{\kappa} \Pi_0^3 = \frac{2}{3} \\ \Pi_0 = & \left(\frac{2}{3} \right)^{\frac{1}{3}} \frac{1}{\theta^{2/3}} \left(\frac{\kappa}{\phi} \right)^{\frac{1}{3}} \end{aligned} \quad (\text{S15})$$

$$\begin{aligned} O(\varepsilon^{1/3}) \Leftrightarrow & 3\Pi_0^2 \Pi_1 - \frac{1}{2} \Pi_0^4 = 0 \\ \Pi_1 = & \frac{1}{6} \Pi_0^2 = \frac{1}{\theta^{4/3}} \left(\frac{\kappa}{\phi} \right)^{\frac{2}{3}} \left(\frac{1}{486} \right)^{\frac{1}{3}} \end{aligned} \quad (\text{S16})$$

$$\begin{aligned} O(\varepsilon^{2/3}) \Leftrightarrow & 3\Pi_0^2 \Pi_2 - 2\Pi_0^3 \Pi_1 + \frac{1}{6} \Pi_0^5 + 3\Pi_0 \Pi_1^2 = 0 \\ \Pi_2 = & \frac{2}{3} \Pi_0 \Pi_1 - \frac{1}{18} \Pi_0^3 - \frac{\Pi_1^2}{\Pi_0} = \frac{1}{54\theta^2} \frac{\kappa}{\phi} \end{aligned} \quad (\text{S17})$$

Using results of Eq. (S15), Eq. (S16), Eq. (S17), $\gamma = 2/3$ and $\alpha = 1/3$ for Eq. (S12) then we have a following result,

$$\Pi = \frac{\kappa}{54\phi\theta^2} + \left(\frac{\kappa^2}{486\phi^2\theta^3} \right)^{\frac{1}{3}} \eta^{\frac{1}{6}} + \left(\frac{2\kappa}{3\phi} \right)^{\frac{1}{3}} \eta^{\frac{1}{3}} \quad (\text{S18})$$

which corresponds to the Eq. (7).

THE TIME EVOLUTION OF DEFORMATION

In the model which I developed in the paper assumes $\frac{d\delta}{dt} = v_i$ though the actual speed of deformation is time-dependent. However, one can observe that the initial deformation speeds corresponds to the impact-velocity which persists for a while, then finally it steeply goes down (see Fig. S2). The region in which the speed of deformation is constant is observed in both viscoelastic and elastic impact. Therefore, it is expect that the main contributions is due to $\frac{d\delta}{dt} = v_i$. Furthermore, if we assume that the actual behavior can be described as $\frac{d\delta}{dt} = v_i + f(t)$ and that $f(t)$ can be expanded in regard to t and that it is well ordered, $f(t)$ does not change the result of Eq. (6) as follows.

Assuming $\frac{d\delta}{dt} = v_i + f(t)$ and $f(t)$ can be applied regard with t and $f(t)$ is well ordered, thus $f(t) = O(t)$ in which O is Landau symbol. As the contact time follows the scaling law $t_c \sim \frac{\delta_m}{v_i}$, then E_{MVF} can be rewritten as follows,

$$E_{MVF} = \frac{\pi\mu\phi R\delta_m^2}{h} \left[v_i + O\left(\frac{\delta_m}{v_i}\right) \right] \left[1 - \exp\left(-\frac{E\delta_m}{\mu v_i}\right) \right]. \quad (\text{S19})$$

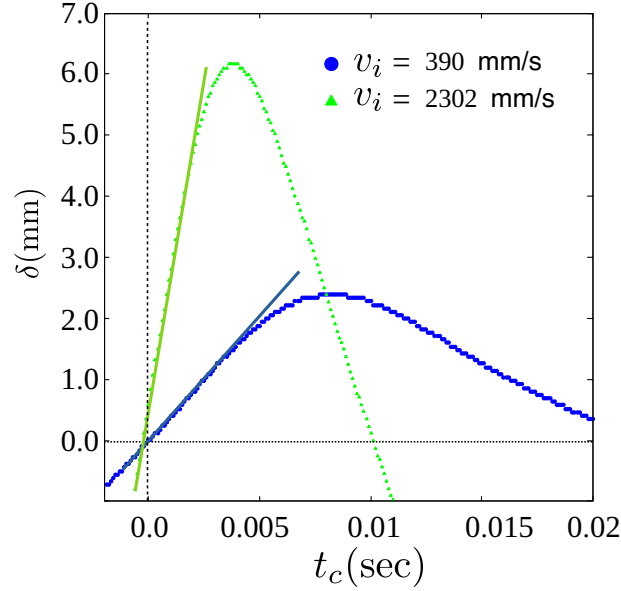


FIG. S2: (Color online) The time evolution of δ of $R = 8.0$ mm with $v_i = 390$ mm/s, $Z = 3.68$ (viscoelastic impact) (●) and $v_i = 2302$ mm/s, $Z = 1.30$ (elastic impact) (▲). The vertical dashed line indicates the moment of contact time and the horizontal dashed line indicates the configuration at $\delta = 0$.

Considering the perturbation of Eq. (S19), Eq. (S11) will be as follows,

$$\frac{2}{3} = \left[\Pi^2 \theta \frac{\phi}{\kappa} \frac{1}{\eta^{1/2}} + O\left(\frac{\Pi^3}{\eta^{3/2}}\right) \right] \left[1 - \exp\left(-\frac{\Pi}{\theta \eta^{1/2}}\right) \right]. \quad (\text{S20})$$

Applying the perturbation of Eq. (S12) for $\gamma = 2/3$ and $\alpha = 1/3$, one obtains

$$\begin{aligned} & \left[\theta^2 \frac{\phi}{\kappa} \varepsilon \Pi^2 + O(\varepsilon^3 \Pi^3) \right] \left\{ \varepsilon \Pi - \frac{1}{2} \varepsilon^2 \Pi^2 + \frac{1}{6} \varepsilon^3 \Pi^3 \dots \right\} = \frac{2}{3} \\ \Leftrightarrow & \theta^2 \frac{\phi}{\kappa} \left(\Pi_0^2 + 2\varepsilon^{1/3} \Pi_1 \Pi_0 + 2\varepsilon^{2/3} \Pi_2 \Pi_0 + \varepsilon^{2/3} \Pi_1^2 + \dots \right) \{ \Pi_0 + \varepsilon^{1/3} \Pi_1 + \varepsilon^{2/3} \Pi_2 + \dots \\ & - \frac{1}{2} \varepsilon^{1/3} \left(\Pi_0^2 + 2\varepsilon^{1/3} \Pi_1 \Pi_0 + 2\varepsilon^{2/3} \Pi_2 \Pi_0 + \varepsilon^{2/3} \Pi_1^2 + \dots \right) + \frac{1}{6} \varepsilon^{2/3} (\Pi_0^3 \dots) \dots \} + O(\varepsilon^{4/3} \Pi_0^4) = \frac{2}{3}. \end{aligned} \quad (\text{S21})$$

As Eq. (S21) shows, the order of ε which derived from $f(t)$ is $O(\varepsilon^{4/3})$, which does not contribute to the third term perturbation.

In the region in which $\frac{d\delta}{dt} = v_i$, the contact time t is surely described as $t = \frac{\delta(t)}{v_i}$. Therefore, the result of perturbation is realized as far as the speed of deformation is constant.

THE RELATION BETWEEN THE DEBORAH NUMBER AND Z

In my model, I utilized the scaling relation $t_c \sim \delta_m/v_i$ [16]. According to the experimental results, the coefficient between t_c and δ_m/v_i is estimated to be : $t_c = 1.90\delta_m/v_i$. Therefore, we have the following conversion between De and Z as $1/\text{De} \simeq 1.90 Z$ (Fig. S3).

[1] G. I. Barenblatt, *Scaling* (Cambridge University Press, 2003) pp.60-65.

[2] G. I. Barenblatt, *Scaling, self-similarity, and intermediate asymptotics* (Cambridge University Press, 1996) pp.86-94.

[3] G. I. Barenblatt, *Flow, Deformation and Fracture* (Cambridge University Press, 2014).

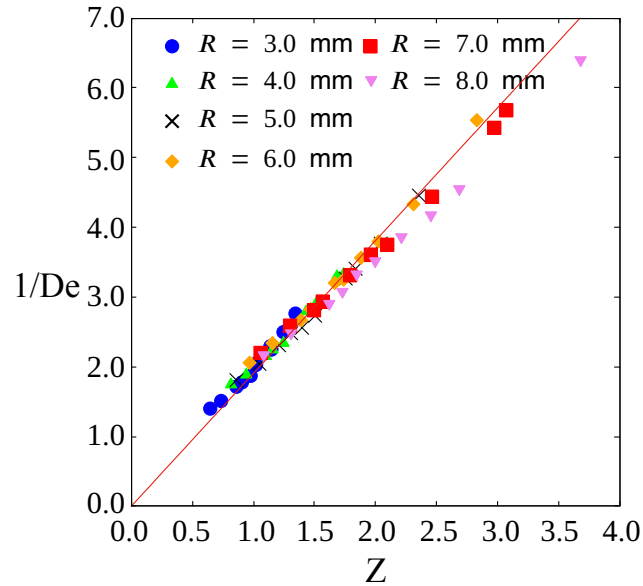


FIG. S3: (Color online) The plots between Z and $1/De$ in which $Z = \frac{E\delta_m}{\mu v_i}$ and $De = \frac{\mu}{Et_c}$. The red line indicates the slope $\simeq 1.90$.

- [4] G. I. Barenblatt and Ya. B. Zeldovich, Self-similar solutions as intermediate asymptotics, *Ann. Rev. Fluid Mech.* **4**, 285 (1972).
- [5] See Refs. [1] (pp. 91-93), [2] (pp.159-160).
- [6] Y. Oono, *The Nonlinear World* (Springer, 2013) Ch.3.
- [7] See Refs. [1] (pp.82-91), [2] (pp.151-159) and [3] (pp. 153-163).
- [8] Ya. B. Zeldovich, The motion of a gas under the action of short term pressure shock. *Sov. Phys. Acoustics*, **2**, 25 (1956).
- [9] See Refs. [1] Ch.3 and [2] Ch.3, 4.
- [10] N. Goldenfeld, *Lecture On Phase Transitions And The Renormalization Group* (Addison-Wesley Publishing Company, 1992) Ch.10.
- [11] N. Goldenfeld, O. Martin and Y. Oono, Intermediate asymptotics and renormalization group theory, *J. Sci. Comput.* **4**, 355 (1989).
- [12] G. I. Barenblatt and L. R. Botvina, Incomplete similarity of fatigue in a linear range of crack growth, *Fatigue Eng. Mater. Struct.* **3**, 193 (1981).
- [13] See Refs. [2] Ch. 12, [1] Ch. 7, [3] Ch. 9.
- [14] B. B. Mandelbrot, *The fractal geometry of nature* (Macmillan, 1983).
- [15] M. H. Holmes, *Introduction to Perturbation Methods* (Springer 2nd ed., 2013) pp.22-27.
- [16] K. L. Johnson, *Contact mechanics* (Cambridge University Press, 1985). p. 353.